

Disturbance-Resistant Control Method for PWM Rectifiers with Proportional-Integral Compensator

Lixin Kuang^{1,*}, Xiaodong Xu¹, Weiping Zhu¹, Jinsong Jia², Guofeng Liu², and Yingjiao Zhang²

¹State Grid Jiangsu Electric Power Co., Ltd., Nanjing 210024, China

²Nanjing Power Supply Company, State Grid Jiangsu Electric Power Co., Ltd., Nanjing 210024, China

ABSTRACT: Subjected to external interference, the input current of a voltage source pulse width modulation (PWM) rectifier distorts, leading to fluctuation in the dc bus voltage. In order to suppress current distortion and DC voltage fluctuation caused by disturbance, a disturbance-resistant control strategy for the PWM rectifiers is proposed. The mathematical model of the conventional double closed-loop control system is built, and the disturbance compensation mechanism is investigated. In addition, the design procedure of the proportional-integral compensator (PIC) is provided. To validate the proposed method, simulation and experiment are considered. The results show that low input current distortion and high bus voltage stability can be realized using the proposed method under the condition of disturbance. The control method is simple and easy to implement in the practical application.

1. INTRODUCTION

Due to controllable bus voltage, high power factor, and reversible energy flow [1–3], voltage source pulse width modulation (PWM) rectifiers have been widely used in the modern smart grid construction such as new energy generation, active power filtering, and energy storage systems [4–7].

Generally, double closed-loop vector control is used as the conventional method of controlling a PWM rectifier [8–10]. However, the influence of the external interference cannot be effectively suppressed with this method, which leads to input current distortion and dc bus voltage fluctuation. The performance of the PWM rectifier is severely affected [11–14]. Consequently, the conventional method is not suitable for the modern smart grid construction [15–17]. Many studies have been conducted on the anti-disturbance control of double closed-loop PWM converter. In [18], based on an extended state observer, a nonsingular terminal sliding mode control method for PWM rectifier is proposed. By designing the observer, the impacts of nonlinear loads, external interference, and parameter perturbations are suppressed in real time. The stability of the system to disturbance will be enhanced. Based on a quasi-resonant extended state observer, a predictive current control strategy is presented in [19]. The system disturbance and grid current on the two-phase stationary coordinate are estimated by the observer. Then, on the basis of deadbeat predictive control principle, the required control output at next moment is calculated. With this approach, the robust control of electrical parameter variations can be achieved, and the effect of measured noise is suppressed. In [20], based on a fractional-order linear extended state observer, an active disturbance suppression control method for a PWM grid-connected rectifier is proposed. The fractional-order linearly expanding state observer is used to es-

timate the system disturbance. Combining it with linear active disturbance suppression control, the compensation of the external interference is enabled. Based on an extended Kalman filter, a disturbance observer is proposed to accurately observe and estimate the grid voltage in [21]. With this method, fast current control can be achieved under the severe grid voltage distortion. In [22], to control the AC/DC matrix converter in the presence unbalanced grid voltage, a simplified model predictive control (S-MPC) method is presented. By simplifying the prediction process, the computational burden of conventional model predictive control (C-MPC) can be significantly reduced. Though anti-interference performance can be realized with the above methods, the parameters are numerous, and the control algorithms are complex.

This study aims to enhance the anti-interference capability of PWM rectifiers while reducing the implementation difficulty of the method. Hence, we fully utilize the advantages of the simple principle and strong adaptability of the proportional integral controller and propose a proportional integral disturbance compensation control method for PWM rectifiers. The main work and contributions of this study can be summarized as follows:

- (1) A mathematical model of PWM rectifier was constructed, and the dual closed-loop control process was clarified, laying a solid foundation for further clarifying the working mechanism of the system.
- (2) The interference compensation mechanism of the proportional-integral compensator (PIC) was analyzed, and based on the capture and characterization of interference signals, a PIC was designed to suppress interference signals, effectively improving the system's anti-interference ability.
- (3) A PIC based control system was established, and the effectiveness and superiority of the proposed method in in-

* Corresponding author: Lixin Kuang (kuanglx1982@163.com).

terference suppression were demonstrated through simulation and physical platforms.

- (4) This study improves the operational quality of PWM converters, enhances their robustness, and contributes to improving power quality.

2. MATHEMATICAL MODELING OF PWM RECTIFIER

The PWM rectifier is shown in Fig. 1. E_{ga} , E_{gb} , and E_{gc} are the grid voltages; i_a , i_b , and i_c are the grid currents; v_a , v_b , and v_c are the input voltages; R and L are the equivalent resistance and filter inductance, respectively; C is the dc-side capacitor; and R_L is the load.

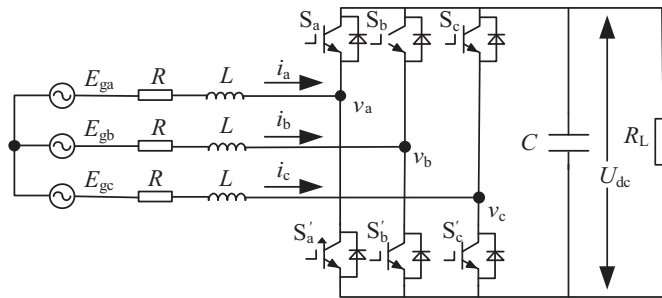


FIGURE 1. Main circuit topology of voltage source PWM rectifier.

The mathematical model of three-phase voltage type PWM converter based on an abc coordinate system contains time-varying parameters, which increase the difficulty of analyzing its control strategy. In the mathematical model based on the dq coordinate system, the AC time-varying parameters are transformed into constant terms that rotate synchronously with the fundamental frequency of the power grid, simplifying the design and analysis of the control method. Below is a detailed analysis of the process of transforming the mathematical model of a three-phase voltage type PWM converter from the abc coordinate system to the dq coordinate system.

In the abc coordinate system, N is the center point. The equation of the a-phase circuit can be expressed as

$$L \frac{di_a}{dt} + Ri_a = E_{ga} - (v_{aN} + v_{N0}) \quad (1)$$

When $s_a = 1$, there is $v_{aN} = U_{dc}$; when $s_a = 0$, there is $v_{aN} = 0$. Therefore, we have $v_{aN} = s_a \times U_{dc}$. Thus, Eq. (1) can be rewritten as

$$L \frac{di_a}{dt} + Ri_a = E_{ga} - (s_a U_{dc} + v_{N0}) \quad (2)$$

Similarly, the equations for the b-phase and c-phase circuits can be obtained as

$$\begin{cases} L \frac{di_b}{dt} + Ri_b = E_{gb} - (s_b U_{dc} + v_{N0}) \\ L \frac{di_c}{dt} + Ri_c = E_{gc} - (s_c U_{dc} + v_{N0}) \end{cases} \quad (3)$$

Considering the three-phase symmetry problem, there exists

$$\begin{cases} E_{ga} + E_{gb} + E_{gc} = 0 \\ i_a + i_b + i_c = 0 \end{cases} \quad (4)$$

By combining Eqs. (2), (3), and (4), the following equation can be obtained.

$$v_{N0} = -\frac{U_{dc}}{3} \sum_{j=a,b,c} s_j \quad (5)$$

At the same time, the DC side current i_{dc} can be expressed as

$$\begin{aligned} i_{dc} = & i_a s_a s'_b s'_c + i_b s'_a s_b s'_c + i_c s'_a s'_b s_c + (i_a + i_b) s_a s_b s'_c \\ & + (i_a + i_c) s_a s'_b s_c + (i_b + i_c) s'_a s_b s_c \\ & + (i_a + i_b + i_c) s_a s_b s_c i_a s_a + i_b s_b + i_c s_c \end{aligned} \quad (6)$$

At this point, there are the following relationships on the DC side.

$$C \frac{dU_{dc}}{dt} = i_a s_a + i_b s_b + i_c s_c - \frac{U_{dc}}{R_L} \quad (7)$$

When transitioning from an abc coordinate system to a two-phase stationary coordinate system, the transformation matrix is as follows:

$$C_{abc-\alpha\beta} = \frac{2}{3} \begin{bmatrix} 1 & -\frac{1}{2} & -\frac{1}{2} \\ 0 & -\frac{\sqrt{3}}{2} & \frac{\sqrt{3}}{2} \end{bmatrix} \quad (8)$$

By the above coordinate transformation, the mathematical model of the two-phase stationary coordination system can be obtained as follows:

$$\begin{cases} L \frac{di_\alpha}{dt} = -Ri_\alpha + u_\alpha - u_{c\alpha} \\ L \frac{di_\beta}{dt} = -Ri_\beta + u_\beta - u_{c\beta} \end{cases} \quad (9)$$

where u_α , $u_{c\alpha}$, and i_α are the grid voltage, input voltage, and input current of the rectifier in the α -axis, respectively. u_β , $u_{c\beta}$, and i_β are the grid voltage, input voltage, and input current of the rectifier in the β -axis, respectively.

The PARK transform facilitates the conversion of mathematical models from a two-phase stationary coordinate system to a synchronously rotating dq coordinate system. Consequently, the model of the rectifier within this synchronously rotating framework can be articulated as

$$\begin{cases} L \frac{di_d}{dt} = \omega Li_q - v_d - Ri_d + e_d \\ L \frac{di_q}{dt} = -\omega Li_d - v_q - Ri_q + e_q \end{cases} \quad (10)$$

where e_d , v_d , and i_d are the grid voltage, input voltage, and grid current in the d -axis, respectively. e_q , v_q , and i_q are the grid voltage, input voltage, and grid current in the q -axis, respectively.

Following the implementation of feedforward decoupling control, the voltages along the dq axis on the AC side can be expressed as

$$\begin{cases} v_d = -\left(k_{ip} + \frac{k_{ii}}{s}\right) (i_d^* - i_d) + \omega Li_q + e_d \\ v_q = -\left(k_{ip} + \frac{k_{ii}}{s}\right) (i_q^* - i_q) - \omega Li_d + e_q \end{cases} \quad (11)$$

where k_{ip} and k_{ii} are the current control ratio and integral coefficient, respectively; i_d^* and i_q^* are command currents in the d -axis and q -axis which can be expressed as

$$\begin{cases} i_d^* = (k_{up} + \frac{k_{ui}}{s})(U_{dc}^* - U_{dc}) \\ i_q^* = 0 \end{cases} \quad (12)$$

where k_{up} and k_{ui} represent the voltage control ratio and integration coefficient, respectively; U_{dc} and U_{dc}^* are the actual value and reference value of the bus voltage, respectively.

3. MECHANISM OF DISTURBANCE COMPENSATION AND DESIGN OF PIC

3.1. Analysis of Disturbance Compensation Mechanism

Figures 2(a) and (b) show the ideal linear system and the linear system with disturbance compensation, respectively.

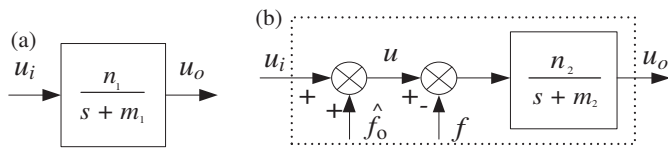


FIGURE 2. First order linear system. (a) Ideal system. (b) \hat{f}_0 compensation linear system under disturbance condition.

From the relationship between the variables in Figs. 2(a) and (b), the first-order differential form of the output in the system can be written as follows

$$\dot{u}_o = -m_1 u_o + n_1 u_i \quad (13)$$

$$\dot{u}_o = -m_2 u_o + n_2 (u - f) \quad (14)$$

where u_i is the actual input; u is the equivalent input; \dot{u}_o is the first derivative of the output u ; f is the external interference; m_1 and n_1 are the nominal parameters ($m_1 > 0, n_1 > 0$); m_2 and n_2 are the actual parameters ($m_2 > 0, n_2 > 0$).

Considering the impact of external interference and parameter uncertainty on the system, the external interference and parameter uncertainty are uniformly represented as the aggregate disturbance f_o , and its formula can be represented as

$$f_o = \frac{(m_1 - m_2)u_o - (n_1 - n_2)u + n_2 f}{n_1} \quad (15)$$

According to Fig. 2(b), the following relationship can be observed.

$$u = \hat{f}_o + u_i \quad (16)$$

where \hat{f}_o is the compensation term.

The design purpose of PIC is to make the final output of the system after it is affected by PIC consistent with the output of the system without interference, that is, to make Eq. (13) and Eq. (14) equivalent.

$$-m_2 u_o + n_2 (u - f) = -m_1 u_o + n_1 u_i \quad (17)$$

Convert the parameters in Eq. (14) to nominal parameters, which can be expressed

$$\dot{u}_o = -m_1 u_o + n_1 (u - f_o) \quad (18)$$

Substituting (16) into (17), it can be obtained that

$$-m_2 u_o + n_2 (u_i + \hat{f}_o - f) = -m_1 u_o + n_1 u_i \quad (19)$$

In the case of slow variations of the lumped disturbance, the differential term of the compensation term when the system is fully compensated is $\dot{\hat{f}}_o \approx 0$. From Eq. (19), it can be deduced that

$$k \dot{\hat{f}}_o = m_2 u_o - n_2 (u_i + \hat{f}_o - f) - m_1 u_o + n_1 u_i \quad (20)$$

where k is a variable and tends towards infinity.

By combining Eqs. (14), (16), and (20), it can be obtained that

$$\frac{k \dot{\hat{f}}_o}{n_1} = \frac{-\dot{u}_o - m_1 u_o + n_1 u - n_2 f \hat{f}_o}{n_1} \quad (21)$$

Combining Eqs. (18) and (21), it can be obtained that

$$\frac{k}{n_1} \dot{\hat{f}}_o = f_o - \hat{f}_o \quad (22)$$

Equation (22) shows the relationship between the lumped disturbance and the compensation term when the disturbance compensation is achieved. Therefore, the compensator is designed as follows

$$\dot{\hat{f}}_o = g (f_o - \hat{f}_o) \quad (23)$$

where g is the gain of the compensator.

After compensation, the system output when being affected by external interference is equal to the result of the system in the normal operation. Thus, the disturbance can be inhibited.

3.2. Design of PIC

To design the PIC, Eq. (18) and Eq. (23) are combined, and it can be obtained that

$$\dot{\hat{f}}_o = g (-\dot{u}_o - m_1 u_o + n_1 u - n_1 \hat{f}_o) / n_2 \quad (24)$$

To further simplify the formula, define the variable λ as

$$\lambda = g u_o / n_1 + \hat{f}_o \quad (25)$$

Hence, it can be obtained that

$$\dot{\lambda} = g \left[u - \lambda + \frac{1}{n_1} (-m_1 + g) u_o \right] \quad (26)$$

In the conventional control, the output voltage is regulated by the PI controller, which enables the control of the d - q axis current. The inputs of the system are the outputs of the PI controller v_{dpi} and v_{qpi} , and the outputs of the system are i_d and i_q . Taking the d -axis as an example, combining Eq. (25) and Eq. (26), the compensator can be further derived as follows

$$\begin{cases} \dot{\lambda} = -k_1 i_d + k_2 u_d \\ \hat{f}_o = -k_3 i_d + \lambda \end{cases} \quad (27)$$

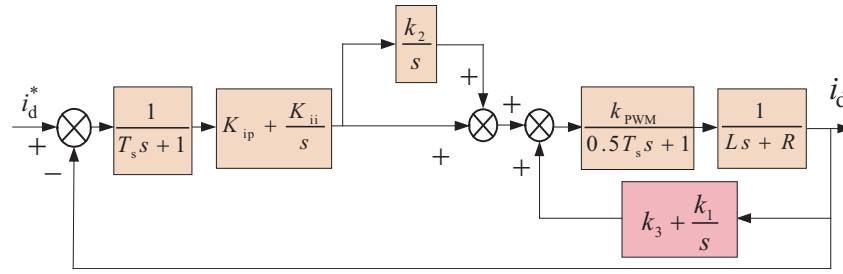


FIGURE 3. Control block diagram of d-axis in current inner loop.

where \hat{f}_o represents the voltage compensation; k_1 , k_2 , and k_3 are constant coefficients; u_d is the output voltage of the PI controller in the d -axis of the current inner loop.

Figure 3 is the current inner loop d -axis control block diagram. T_s represents the sampling time, and k_{PWM} is the equivalent gain of the three-phase voltage type PWM converter.

The open-loop transfer function of the current inner loop can be obtained from Fig. 3 as follows

$$G(s) = \frac{1}{T_s s + 1} \times \left(k_{ip} + \frac{k_{ii}}{s} \right) \times \left(1 + \frac{k_2}{s} \right) \times \frac{1}{(0.5 T_s s + 1) \times (L s + R) - k_2 \times \left(k_3 + \frac{k_1}{s} \right)} \quad (28)$$

By substituting $k_{ii} = k_{ip}/\tau_i$ into Eq. (28), it can be obtained that

$$G(s) = \frac{1}{T_s s + 1} \times \left(1 + \frac{1}{\tau_i s} \right) \times \frac{k_{ip}(s + k_2)}{s(0.5 T_s s + 1)(L s + R) - k_2(s k_3 + k_1)} \quad (29)$$

Generally, to reduce the order in the dual closed-loop control system, τ_i is usually defined as

$$\tau_i = L/R \quad (30)$$

By substituting Eq. (30) into Eq. (29), it can be obtained that

$$G(s) = \frac{1}{T_s s + 1} \times \frac{1}{L s} \times \frac{k_{ip}(L s + R)(s + k_2)}{s(0.5 T_s s + 1)(L s + R) - k_2(s k_3 + k_1)} \quad (31)$$

In order to further reduce the order and form negative feedback in the latter half, the following parameter values are given as

$$\begin{cases} k_1 = -gR \\ k_2 = g \\ k_3 = -gL \end{cases} \quad (32)$$

At this point, the stable controller parameters are transformed into the following equation.

$$\begin{cases} \dot{\lambda} = gRi_d + gu_d \\ \hat{f}_o = \lambda + Lgi_d \end{cases} \quad (33)$$

Therefore, the compensation term provided by PIC in the system can be represented as

$$\hat{f}_o = -gLi_d + \int_0^t (-gRi_d + gu_d)d\tau \quad (34)$$

4. CONSTRUCTION OF THE CONTROL SYSTEM

Figure 4 illustrates the structure of the proposed controller. Based on the conventional control of the PWM rectifier, the actual values of current and the outputs of the PI controllers in the d - q axis are used as the inputs for two PIC controllers. The outputs of two PIC controllers are added to the corresponding outputs of PI controller in the d - q axis. Considering the feed-forward compensation and coupling components, the final output voltage is obtained. The switching signal for the power control devices is acquired by space vector pulse width modulation.

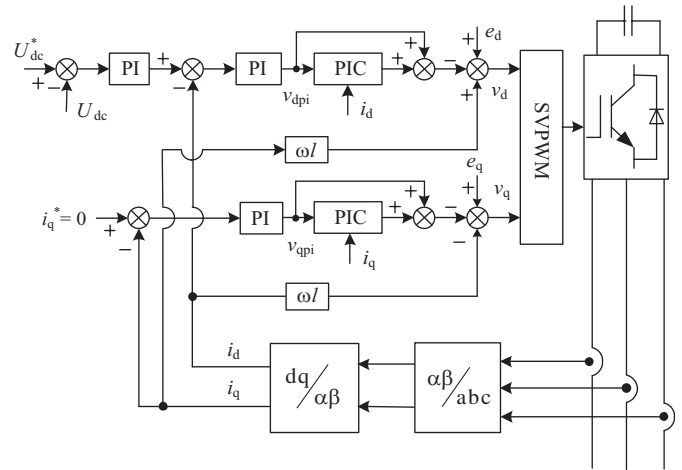


FIGURE 4. Structure block diagram of the proposed method.

5. SIMULATION AND ANALYSIS

To validate the feasibility of the proposed approach, simulation analysis is conducted. The parameters are shown in Table 1.

In the conventional control of the PWM rectifier, d -axis is generally used to control the active power and bus voltage. Consequently, to validate the performance, the sinusoidal interference signal with the frequency of 50 rad/s is added to the d -axis.

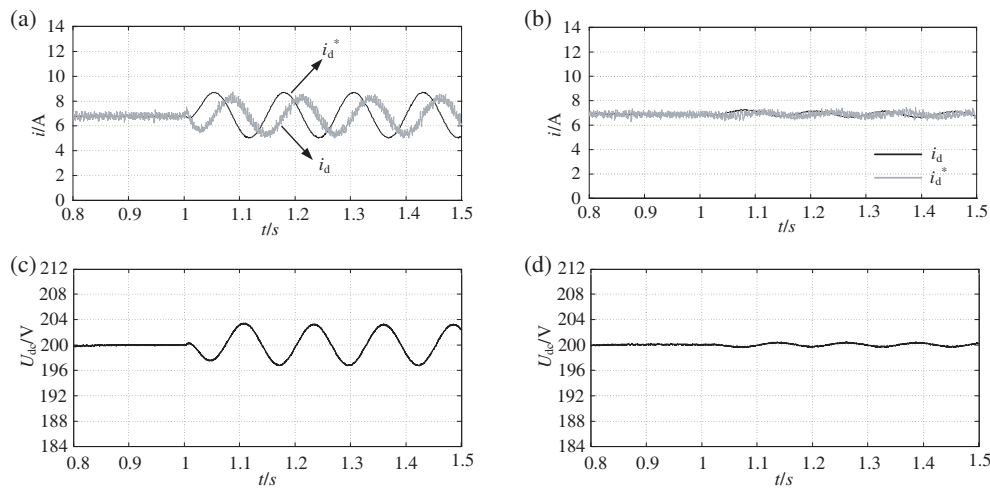


FIGURE 5. d -axis current and dc bus voltage in the presence of interference. (a) d -axis current when using the conventional method. (b) d -axis current when using the proposed method. (c) DC bus voltage when using the conventional method. (d) DC bus voltage when using the proposed method.

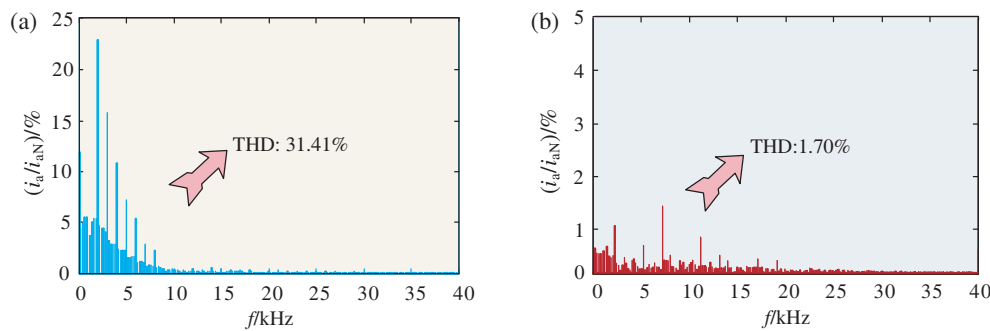


FIGURE 6. Spectrum of a-phase current under different strategies under interference conditions. (a) Conventional method. (b) Proposed method.

TABLE 1. Main parameters of PWM rectifier.

Parameters	Values	Parameters	Values
Rated power	1 kW	Bus voltage	20 V
Grid frequency	50 Hz	Input inductance	8 mH
Input voltage	12 V	Bus capacitor	2350 μ F

Figure 5 shows the d -axis current and dc bus voltage of the PWM rectifier using the conventional control and proposed control method. During the operation, the interference signal is added to the d -axis at $t = 1$ s. Figs. 5 (a) and (c) show the current and voltage controlled by the conventional method, respectively. Figs. 5(b) and (d) illustrate the current and voltage controlled by the proposed method, respectively.

Figure 5(a) provides the waveform of d -axis current using the conventional method in the presence of interference. As can be seen, current fluctuation of the PWM rectifier is about 3 A. Meanwhile, since the current fluctuation causes the fluctuation of the bus voltage, the reference value of the d -axis current i_d^* also exhibits a large fluctuation. As a result, fluctuation is observed in the calculated reference value. In contrast, it is seen from Fig. 5(b) that the disturbance can be compensated by the compensator in the presence of interference when the proposed method is used. Thus, more stable d -axis current is obtained,

and there is no obvious fluctuation in the reference value. As shown in Fig. 5(c), in the presence of sinusoidal disturbance, the dc bus voltage U_{dc} of the PWM rectifier exhibits a fluctuation about 6 V when the conventional method is used. By comparison, the stability of the bus voltage is significantly enhanced with the proposed method, as illustrated in Fig. 5(d).

Figure 6 illustrates the a-phase current spectrum of a three-phase voltage type PWM converter under interference conditions. This figure compares the performance of the conventional method with that of the proposed method, providing insights into their respective effectiveness in mitigating interference effects.

Upon examination of Fig. 6(a) and Fig. 6(b), a striking contrast is evident in the harmonic performance of the three-phase voltage type PWM converter under two distinct control methodologies. Specifically, when the conventional method is employed, the a-phase current exhibits a total harmonic distortion (THD) of 34.41%. In stark contrast, the implementation of the proposed method significantly reduces this figure to a mere 1.70% for the same a-phase current. This dramatic reduction not only underscores the superior anti-interference capabilities of the proposed approach but also unequivocally highlights its efficacy in enhancing power quality, thereby affirming its potential as a preferable solution for mitigating harmonic distortions in such systems.

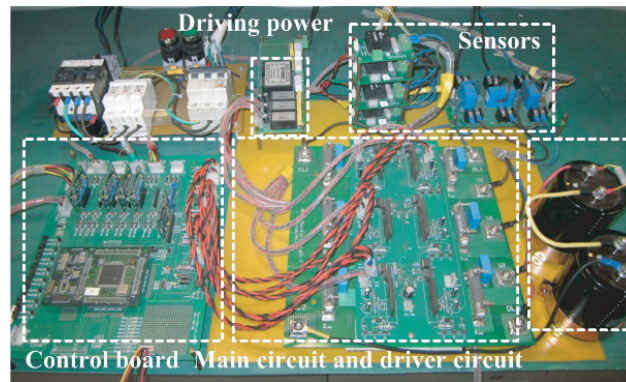


FIGURE 7. Experimental platform.

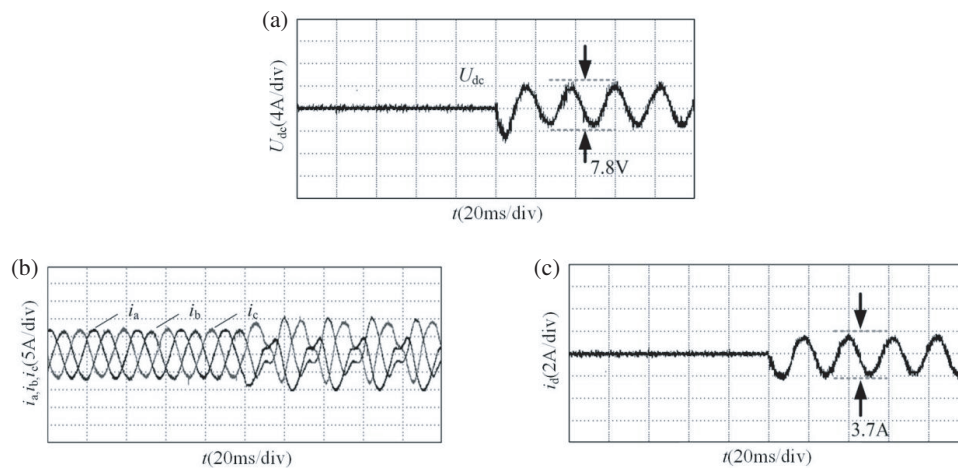


FIGURE 8. Experimental waveforms under interference conditions when using the conventional control method. (a) DC bus voltage. (b) Grid current. (c) d -axis current.

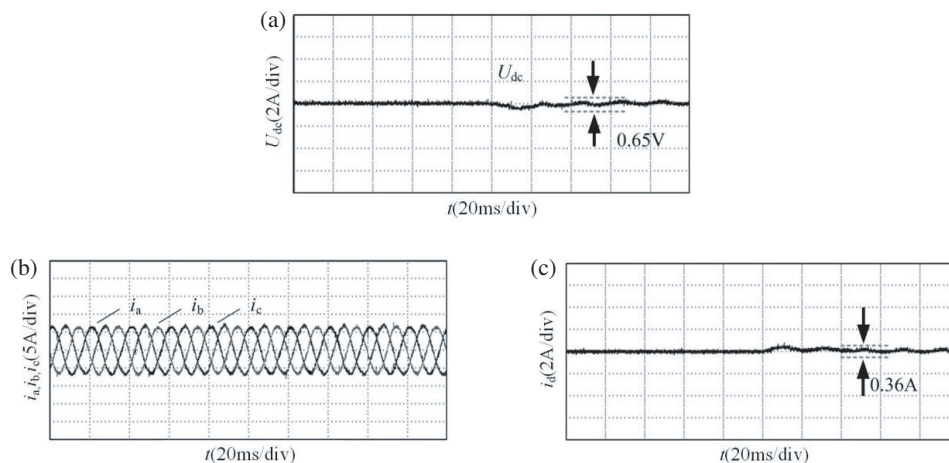


FIGURE 9. Experimental waveforms under interference conditions when using the proposed control method. (a) DC bus voltage. (b) Grid current. (c) d -axis current.

6. EXPERIMENTAL VERIFICATION

Figure 7 shows the experimental prototype of the PWM rectifier. The experimental parameters are consistent with the simulation. The devices employed in the experimental plat-

form's circuit are detailed in Table 2. The main circuit features the FGL40N120AND as its fully controlled IGBT switching device, while the driving circuit incorporates the M57962AL driving module. Control of the system is facilitated by the

TABLE 2. Device used in circuit of experimental platform.

Circuit	Device type	Circuit	Device type
Main circuit	FGL40N120AND	Current detection circuit	LA50P
Drive circuit	M57962AL	Voltage detection circuit	VSM025A
Control circuit	TMS320F28335	Butterworth circuit	MAX274

TMS320F28335 DSP. For current detection, an LA50P current sensor is utilized, and voltage detection employs a VSM025A voltage sensor. Additionally, a Butterworth filter circuit is centered around the MAX274 chip as its primary component.

Figures 8 and 9 show the dc bus voltage, grid side current, and d -axis current of the PWM rectifier under the disturbance. The PI conventional control and the proposed control method are used, respectively. Fig. 8 illustrates that the bus voltage fluctuates significantly in the presence of interference, and the fluctuation of the amplitude is 7.8 V. Besides, the grid input current is highly distorted, and the performance of system is obviously affected. Comparatively, Fig. 9 shows that the bus voltage fluctuation can be highly reduced and that the steady-state fluctuation amplitude is 0.65 V when the proposed method is used. From the above comparison, the proposed method has an excellent anti-disturbance performance.

7. CONCLUSION

Modern smart distribution network construction requires a high level of robustness in the performance of PWM rectifiers. The existing anti-disturbance control algorithms for the PWM rectifiers are very complex. To solve the problem, a novel proportional-integral method with simple structure is proposed for disturbance compensation. By introducing a proportional-integral compensator into a conventional double closed-loop control structure, the real-time compensation of external interference is realized, and the influence of disturbance is reduced with this method. The results show that dc bus voltage fluctuation and grid input current distortion can be effectively suppressed with the proposed method in the case of external interference, significantly improving the quality of the grid current and the stability of bus voltage. Superior anti-interference performance has been realized. Although the anti-interference method based on a proportional integral compensator proposed in this paper has shown significant superiority under grid balance conditions, it should be pointed out that this method mainly targets the external interference problem under grid balance state. In practical applications, the grid may encounter unbalanced situations, such as single-phase grounding faults and asymmetric loads, which will have different effects on the performance of PWM rectifiers. Therefore, future research can further explore how to effectively expand or improve existing methods under grid imbalance conditions to enhance their robustness and adaptability under different grid conditions.

ACKNOWLEDGEMENT

This work was supported by the Business Research Project of State Grid Jiangsu Electric Power Co., Ltd. (2024-1-28, Research on the Implementation Path and Key Strategies of Modern Smart Distribution Network).

REFERENCES

- [1] Song, T., Y. Zhang, F. Gao, C. Xu, and X. Zhu, "Data-driven adaptive negative sequence current control method for PWM rectifier under unbalanced grid," *IEEE Transactions on Power Electronics*, Vol. 39, No. 4, 4771–4780, 2024.
- [2] Le, V.-T. and H.-H. Lee, "An enhanced model-free predictive control to eliminate stagnant current variation update for PWM rectifiers," *IEEE Journal of Emerging and Selected Topics in Power Electronics*, Vol. 9, No. 6, 6804–6816, 2021.
- [3] Spadacini, G., F. Grassi, and S. A. Pignari, "Modelling and simulation of conducted emissions in the powertrain of electric vehicles," *Progress In Electromagnetics Research B*, Vol. 69, 1–15, 2016.
- [4] Mahmood, A. S., "Enhancing performance of photovoltaic pump systems in remote areas using a sliding mode technique for maximum power point tracking," *Progress In Electromagnetics Research B*, Vol. 104, 131–146, 2024.
- [5] Wang, M., H. Wang, Y. Shi, M. Shen, and J. Song, "A modified sliding-mode controller-based mode predictive control strategy for three-phase rectifier," *International Journal of Circuit Theory and Applications*, Vol. 48, No. 10, 1564–1582, 2020.
- [6] Zhang, Z., J. Chang, M. Li, P. Zhang, and W. Zhang, "Optimization of bus capacitance of six-phase permanent magnet power generation system based on PWM modulation," *Progress In Electromagnetics Research C*, Vol. 138, 261–273, 2023.
- [7] Fu, C., C. Zhang, G. Zhang, C. Zhang, and Q. Su, "Finite-time command filtered control of three-phase AC/DC converter under unbalanced grid conditions," *IEEE Transactions on Industrial Electronics*, Vol. 70, No. 7, 6876–6886, 2023.
- [8] Nguyen, M. H., S. Kwak, and S. Choi, "Model predictive based direct power control method using switching state preference for independent phase loss decrease of three-phase pulsewidth modulation (PWM) rectifiers," *IEEE Access*, Vol. 12, 5864–5881, 2024.
- [9] Fu, C., C. Zhang, G. Zhang, and Q. Su, "Finite-time adaptive fuzzy control for three-phase PWM rectifiers with improved output performance," *IEEE Transactions on Circuits and Systems II: Express Briefs*, Vol. 70, No. 8, 3044–3048, 2023.
- [10] Kakkar, S., T. Maity, R. K. Ahuja, P. Walde, R. K. Saket, B. Khan, and S. Padmanaban, "Design and control of grid-connected PWM rectifiers by optimizing fractional order PI controller using water cycle algorithm," *IEEE Access*, Vol. 9, 125 941–125 954, 2021.
- [11] Al Razeqi, M., R. Errouissi, M. Debouza, and H. Shareef, "Mitigation of 2ω -ripple in dc-link voltage of PWM rectifiers under

- unbalanced grid conditions,” *IEEE Transactions on Industry Applications*, Vol. 59, No. 6, 7608–7622, 2023.
- [12] Gao, X., D. Zhou, A. Anvari-Moghaddam, and F. Blaabjerg, “Stability analysis of grid-following and grid-forming converters based on state-space modelling,” *IEEE Transactions on Industry Applications*, Vol. 60, No. 3, 4910–4920, 2024.
- [13] Song, T., Y. Zhang, F. Gao, X. Zhu, J. Shan, and Z. Kong, “Power model free voltage ripple suppression method of three-phase PWM rectifier under unbalanced grid,” *IEEE Transactions on Power Electronics*, Vol. 37, No. 11, 13 799–13 807, 2022.
- [14] Le, V.-T. and H.-H. Lee, “Grid-voltage sensorless model-free predictive current control for PWM rectifiers with measurement noise suppression,” *IEEE Transactions on Power Electronics*, Vol. 37, No. 9, 10 681–10 697, 2022.
- [15] Qamar, H., H. Qamar, N. Korada, and R. Ayyanar, “240°-clamped PWM applied to transformerless grid connected PV converters with reduced common mode voltage and superior performance metrics,” *IEEE Open Journal of Power Electronics*, Vol. 3, 153–167, 2022.
- [16] Zarei, S. F., H. Mokhtari, M. A. Ghasemi, S. Peyghami, P. Davari, and F. Blaabjerg, “Control of grid-following inverters under unbalanced grid conditions,” *IEEE Transactions on Energy Conversion*, Vol. 35, No. 1, 184–192, 2020.
- [17] Gui, Y., F. Blaabjerg, X. Wang, J. D. Bendtsen, D. Yang, and J. Stoustrup, “Improved dc-link voltage regulation strategy for grid-connected converters,” *IEEE Transactions on Industrial Electronics*, Vol. 68, No. 6, 4977–4987, 2021.
- [18] Yu, H., Z. Kang, and P. He, “Extended state observer based non-singular terminal sliding mode control for voltage source converter station with uncertain disturbances,” *IEEE Access*, Vol. 9, 122 228–122 235, 2021.
- [19] Yang, X., H. Hu, H. Hu, Y. Liu, and Z. He, “A quasi-resonant extended state observer-based predictive current control strategy for three-phase PWM rectifier,” *IEEE Transactions on Industrial Electronics*, Vol. 69, No. 12, 13 910–13 917, 2022.
- [20] Pan, Z., X. Wang, Z. Zheng, and L. Tian, “Fractional-order linear active disturbance rejection control strategy for grid-side current of PWM rectifiers,” *IEEE Journal of Emerging and Selected Topics in Power Electronics*, Vol. 11, No. 4, 3827–3838, 2023.
- [21] Liao, H., X. Zhang, and Z. Ma, “Robust dichotomy solution-based model predictive control for the grid-connected inverters with disturbance observer,” *CES Transactions on Electrical Machines and Systems*, Vol. 5, No. 2, 81–89, 2021.
- [22] Nguyen, T.-L. and H.-H. Lee, “Simplified model predictive control for AC/DC matrix converters with active damping function under unbalanced grid voltage,” *IEEE Journal of Emerging and Selected Topics in Power Electronics*, Vol. 8, No. 3, 2907–2917, 2020.